Marble provenance designation with Object Based Image Analysis: State-of-the-art rock fabric characterization from petrographic micrographs

Peter HOFMANN[1)*)], Robert MARSCHALLINGER[1)], Michael UNTERWURZACHER[2)3)] & Fritz ZOBL[1)]

[1)] Interfaculty Department of Geoinformatics, University of Salzburg, Schillerstr. 30, 5020 Salzburg, Austria;

[2)] Department of Geography and Geology, University of Salzburg, Hellbrunnerstr. 34, 5020 Salzburg, Austria;

[3)] Institute of Archaeology, University of Innsbruck, Langer Weg 11, 6020 Innsbruck, Austria;

[*)] Corresponding author, peter.hofmann@sbg.ac.at

KEYWORDS

Object Based Image Analysis
Provenance Analysis
Micrographs
Petrography
Marble

Abstract

The designation of marble provenance plays an important role in Cultural History, Archeology and Geosciences in general. In the multidisciplinary approach to explore marble provenance, petrography plays a key role. This paper presents a novel method for automatic image analysis of marble micrographs: Object Based Image Analysis (OBIA), via the incorporation of petrographic expert knowledge, enables the reliable extraction of mineral grains and yields a wealth of quantitative shape and texture measures. A work flow is introduced for extracting mineral shape characteristics from marble micrographs, comprising data acquisition, pre-processing and Object Based Image Analysis. Therefore verifiable parameters and analysis supply marble provenance research particularly for multiple sample analysis in an efficient and timely manner.

Die Bestimmung der Herkunft von Marmoren ist von großer Bedeutung für Kulturgeschichte, Archäologie und allgemein für die Geowissenschaften. Die Petrographie spielt im multidisziplinären Ansatz der Herkunftsbestimmung eine wichtige Rolle. In diesem Artikel wird eine neue Methode zur automatischen Bildanalyse von Marmor Dünnschliffen präsentiert: Objektbasierte Bildanalyse (OBIA) kann petrographisches Expertenwissen in den Analysevorgang einbeziehen und ermöglicht so, neben einer verlässlichen Extraktion von Mineralkörnern, die Darstellung einer Vielzahl von quantitativen Form- und Texturparametern.

Es wird ein Arbeitsablauf zur Extraktion von Formparametern von Calcitkörnern aus Marmordünnschliffen vorgestellt: Datenerfassung, Datenvorverarbeitung und Objektbasierte Bildanalyse. Die Analyse liefert nachvollziehbare Ergebnisse und unterstützt dadurch besonders bei Mehrfachprobenauswertung die zeiteffiziente Herkunftsbestimmung von Marmoren.

1. Introduction

1.1 Marble provenance and its matter for cultural history

Throughout cultural history, marble has had great significance as a building stone, as decorative material and, in particular, as material for statues. Marble production and its use have been documented since the Neolithic (Cramer, 2004). Preindustrial quarrying of marble began in the Mediterranean countries during the Bronze Age. Advanced skills, techniques and tools which presumably developed under Egyptian influence subsequently spread into surrounding regions; large scale marble quarrying was carried out by the Romans in present-

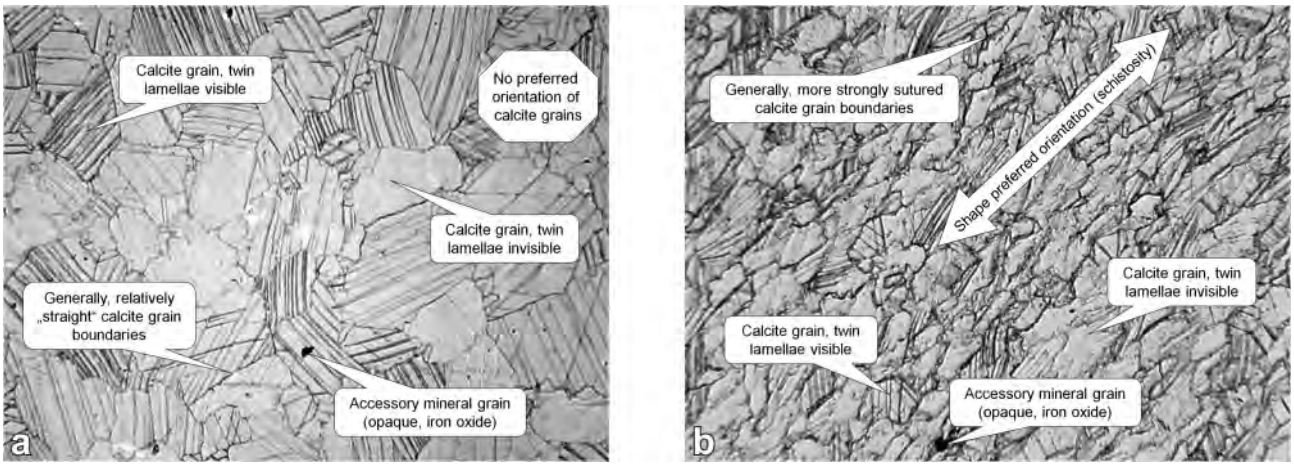

Figure 1: Thin section micrographs (parallel polarizers) of marble samples highlighting some fabric features that are important in provenancing. Figure 1a: isotropic sample LAS13, Figure 1b: schistose sample SPE13. Note that the visibility of twin lamellae depends on the rotation of the thin section relative to the polarizing filters. Image length 0.75mm for both images, see text for details.

day Greece, on the Greek Islands but also in Turkey (Cramer, 2004). Material from these quarries can be found in all parts of the Roman Empire. While the provenance of marble used in modern buildings is mostly well documented, this is rarely the case for historical objects. This is particularly true for white marbles that often look similar, especially from a macroscopic point. Since mainly the pure marbles were extracted from the quarries, characteristic colored zones within the quarries or impurities within single blocks led to a negative selection of these blocks. This is why marble provenance can only rarely be designated by macroscopic criteria alone. On the other hand, knowing the provenance of the material is of utmost importance in archaeology. It helps identifying object togetherness. Sample complexes, identified by stylistic criteria can be verified. Results from provenance studies may prove the extraction of material from a specific quarry at a specific time, it may give an idea on economic relations and travel routes and sometimes also on workshops and settlements.

1.2 Methods of provenance analysis

The importance of Greek and Roman history has led many natural scientists to an interest in these subjects, and it was soon realised that natural sciences are able to provide additional information to assist with historical interpretations. Marble samples from potentially used quarries and from archaeological/historical objects were subject to comparative studies. The first petrographic studies for provenance analysis by Lepsius (1891) were soon followed by many others. Successful provenance studies for classical marbles were published by Craig and Craig (1972), who used stable isotopes of carbon and oxygen. Intense sampling programmes followed in the succeeding years, with many different groups working on the provenance of marbles (Herz, 1988; Gorgoni et al., 2002; Attanasio, 2003; Lazzarini, 2004). Stable isotope studies initially appeared to be a suitable method for differentiating marble occurrences, but the more data accumulated, the broader the isotopic clusters for single quarries and quarry areas were shown to be. An increasing overlap in the data from different areas was revealed.

Evidently, a bundle of marble characteristics have to be taken into account in provenance analysis for obtaining reliable results. These include material-inherent parameters such as petrography, mineralogy, geochemistry and isotopy of samples and their possible quarry areas, as well as additional features such as their Electron Paramagnetic Resonance (EPR is a spectroscopic technique for studying materials with unpaired electrons. In marbles mainly the Mn^{2+} peak in the spectrum can be significant. A detailed description of the method and its use in provenancing marbles is given by Attanasio, 2003) and luminescence spectra. In addition, quarry-specific criteria like the presence of voids, the block sizes, etc. need to be included. The amount of quarrying, the time of quarrying, logistic aspects (such as the distance from archaeological objects), multiple occurrences or quarries in the source region, and the transport possibilities (navigable rivers, roads, etc.) need to be considered. Furthermore the influence of sculptors, their schools and studios, and their experience, together with the origin of builders, political relationships, the importance of the antique objects to the inhabitants and their financial status are of vital interest (Cramer, 2004). Since these details are often unknown, archaeologists and historians consider natural

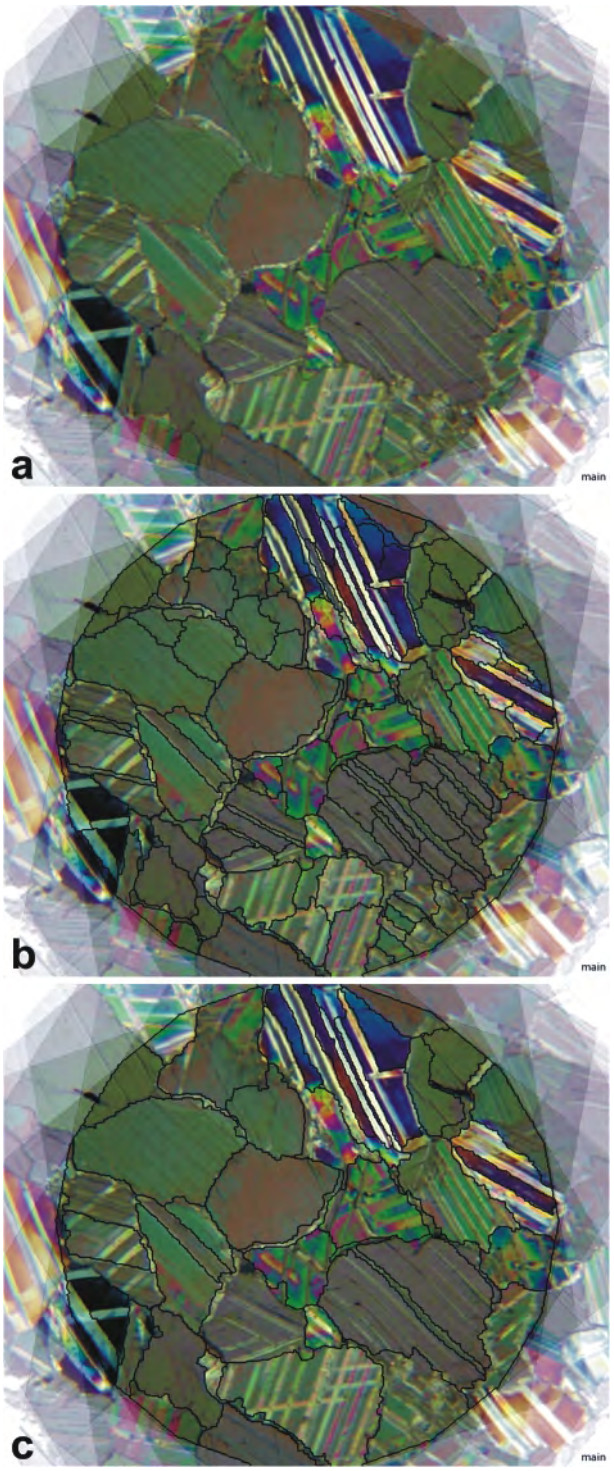

Figure 2: Comparing original micrograph stack and results of two-level segmentation. Figure 2a: original image stack. Figure 2b: base level, MRS1. Figure 2c: top level, MRS 2. Segmentations created using parameters from Table 1. Super imposed to all rotated cross polarized images for reference.

sciences to assist in determining these important parameters. It is this interdisciplinary aspect of provenance analysis that makes it so important and exciting. In the field of provenance analysis in most cases only a combination of the methods mentioned above leads to a successful provenance determination. Apart from the use of stable isotopes of C and O mentioned above, grain size characteristics and particularly grain size and morphological analyses of the carbonate grains gained from thin section analysis play a key role in provenancing marbles. Using methods of Object Based Image Analysis (OBIA) support an automated analysis of thin section images and to incorporate domain expert knowledge. Moreover, OBIA supports the automated delineation of single grains, to analyse their shape and interior fabric properties and finally to deduce typical characteristics of the marble specimen supporting its determination of provenance. At this background the paper demonstrates its application for thin section analysis.

2. Materials and methods

2.1 Thin section analysis of marbles

In marble provenance analysis, petrography is an important issue: the proportions of major minerals (calcite, dolomite) and diverse accessory minerals (mostly quartz, micas, ore minerals), associated grain sizes and grain shapes as well as fabric characteristics like the abundance of preferred grain elongation or schistosity can identify a specific quarry or quarry subarea. Marble petrography – i.e., the mineralogical composition and texture properties – can be conveniently derived from standard (30µm) petrographic thin sections using an optical microscope (Tröger et al., 1982; Higgins, 2006).

Fig.1 shows typical micrographs of marble thin sections: Fig. 1a is a relatively isotropic sample, while Fig. 1b is anisotropic. In the current context, the most important grain shape parameters are the maximum and the mean grain size of the carbonate grains. Since thin section analysis infers the shape parameters of inherently three-dimensional mineral grains from two-dimensional sections, the measures derived are only approximations. In consequence, only a large number of measurements yields representative results: per thin section usually at least 100 long diameters of carbonate grains have to be measured with the microscope. While this approach yields quantitative results, there is no clear standard on gauging the grain size. Going into more detail, also the geometric characteristics of carbonate grains are of major interest: besides grain size and shape, twinning types and the nature of grain boundaries have been successfully used as provenance factors (Unterwurzacher et al., 2005). Grain boundaries can be straight or sutured, with varying amount of suturing. Relying on human observation alone, suturing can be at best described in terms of fuzzy categories such as “straight, weakly sutured or sutured”. Moreover, given that research groups rarely provide information on data acquisition procedures, the findings of different researchers can be related with difficulties only.

Summing up, petrographic microscopy yields important provenance indicators, but the purely human-based approach involves non-documented expert knowledge and is time-consuming, subjective and error-prone. An experienced analyst needs approximately 1 hour for measuring 100 grains. Classical, pixel-based image analysis methods have been adapted to petrographical micrographs and successfully applied in many fields of petrographic microscopy (Bons and Jessell, 1996; Fueten, 1997; Obara and Kozusnikova, 2007). Unfortunately, purely pixel-based image processing methods do not cover extended analysis of grain shapes like suturing or grain neighborhood analysis, which are of interest in the provenancing of classical marbles.

Segmentation	Scale Parameter/Object Size	wshape	wcolor	wcomp	wsmooth
Chessboard	1	-	-	-	-
MRS1	50	0.5	0.5	0.5	0.5
MRS2	200	0.4	0.6	0.2	0.8

Table 1: Parameters used for initial image segmentation.

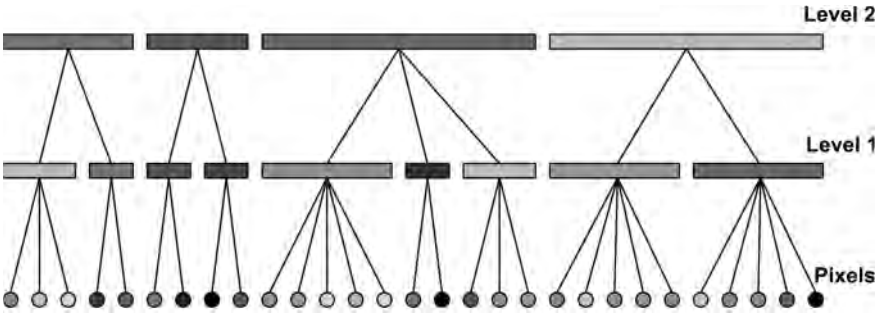

Figure 3: Object hierarchy generated after image segmentation (here with three levels of segmentation). Each higher-level object is connected with its sub-objects and vice versa. For higher-level objects their inner structure can be analyzed by referring to their sub-objects at the next level below.

Segmentation	Scale Parameter/Object Size	wshape	wcolor	wcomp	wsmooth
MRS1	10	0.1	0.9	0.5	0.5

Table 2: Segmentation parameters for the re-segmentation of the base level (MRS 1).

2.2 Marble sample

The marble sample LAS3 originates from the Weisswasserbruch quarry near the village of Laas (Northern Italy). The Laas Marble District is one of the most important marble occurrences of the Eastern Alps (e.g. Unterwurzacher and Obojes, 2012). LAS3 is a white calcitic marble consisting of the rock forming mineral calcite and

traces of accessory minerals, mostly quartz and iron oxides. The marble is fine-grained with weakly sutured grain boundaries. For later comparison with OBIA results, about 100 calcite grains were manually measured in a LAS3 thin section. This yielded a mean grain size of 0.7 mm and a maximum grain size of 1.3 mm.

2.3 Image acquisition

For image acquisition, a Zeiss Photomicroscope 1 with an attached Sony Digital Imaging System (resolution 768*576 pixels, color depth 32bit) was used. The microscope is set up for petrography, with two polarization filters and a rotary stage, enabling the investigation with plan-polarized light as well as with crossed (90°) polarizers.

2.4 Image stacking

To maximize the microscopic information input to OBIA, we combined micrographs acquired at different rotations of the polarization filters. This closely mimics a petrographer's approach to distinguishing minerals in thin section by comparing different rotations of the thin section with respect to parallel and crossed polarization filters. Practically, the procedure was as follows: the microscope rotary stage with the attached sample was step-wise rotated at increments of 20° and each position was acquired in parallel polarized light and with 90° crossed polarizers. Accordingly, from this procedure, a set of 36 images (e.g., each position with parallel and crossed polarizers) was derived. To enable the analysis of all derived images with OBIA, all images had to be co-registered first. That is, each image was back-rotated and shifted to its original relative position. For co-registration we used the images with a rotation angle of 0° as reference images. All other images were first turned back according to their rotation angle and then shifted by individually determined affine transformation functions. The reference points for these functions were selected semi-automatically using the AutoSync module of the software package Erdas Imagine (Erdas, 2011). The co-registered images were used as input data for the following OBIA.

3. Marble Petrography from thin sections using OBIA

3.1 Object based image analysis (OBIA)

OBIA as a method for image analysis has been originally introduced in remote sensing (e.g. Blaschke, 2010). Especially in the light of steadily increasing spatial resolutions of remote sensing platforms, classic methods of pixel based image processing yielded increasingly unsatisfying results. Object based approaches approved to be an alternative (Blaschke and Strobl, 2001). In contrast to pixel based approaches OBIA uses spatially contiguous image objects as the building blocks for image analysis. As a first step in OBIA, image objects are generated from the original image. For the generation of these image objects, a range of so-called image segmentation methods is available. In GIS-Science, image analysis of remote sensing data is widely used to generate or update geo-datasets stored in geo-information systems ("GIS") (Benz et al., 2004; Lang, 2008). Due to the similarity of objects in OBIA with polygons in GIS, OBIA has been regarded as the bridging element between GIS and remote sensing (Blaschke, 2010). In fact, one of the strengths of OBIA is to analyze image objects beyond

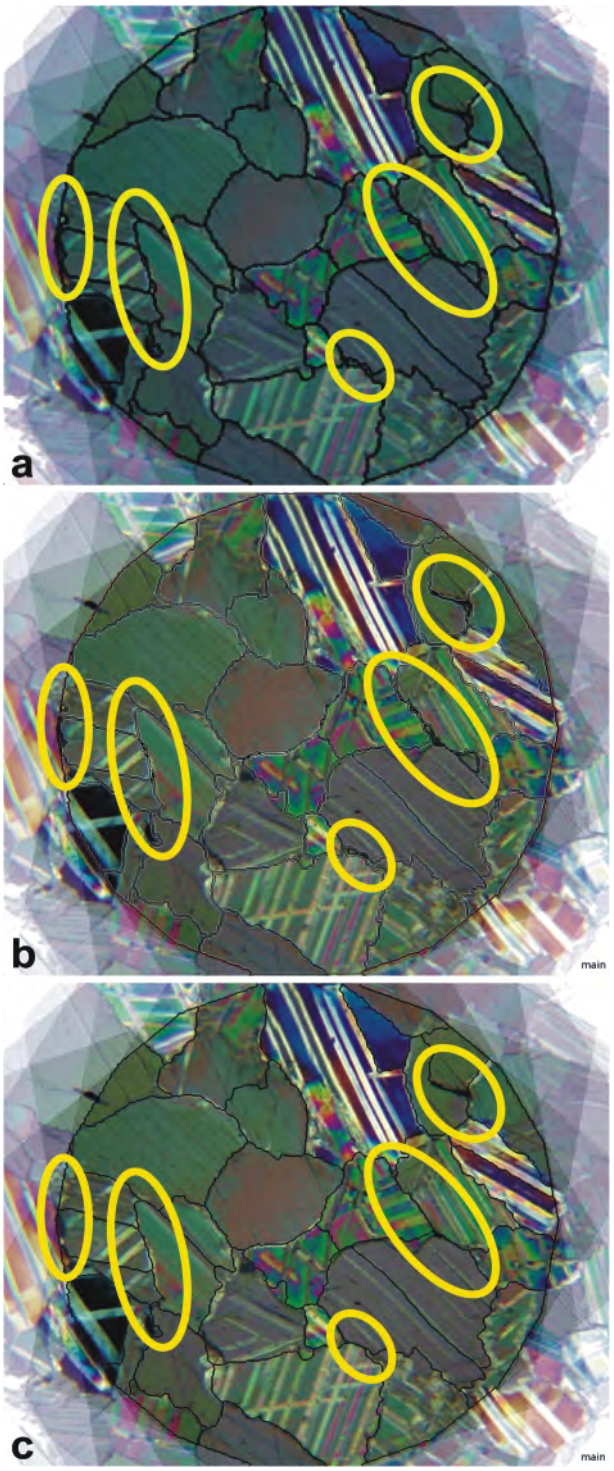

Figure 4: Results of growing and shrinking for enhancing grain boundaries. Ellipses highlight areas with changes to borderlines. Figure 4a: after eliminating elongated objects. Figure 4b: after shrinking the remaining objects. Figure 4c: after growing these back into generated interspaces.

their spectral properties: following the initial image segmentation, the resulting image objects can be analyzed and merged into new image objects based on shape properties and spatial relationships (e.g., neighbourhoods, distances, shared borders). Additionally, spatial hierarchical relationships between image objects can be considered, such as “being-part-of” or “consists-of” relationships. Mostly, the initial image segmentation is only sub-optimal in terms of representing objects of interest and it is necessary to stepwise enhance the initial segmentation results by focusing on dedicated objects. Sometimes it may be necessary to re-assign objects according to their changed properties. In consequence, OBIA is considered as an iterative process, starting with global processing and analysis steps and ending up with local operations (Baatz et al., 2008). The so-called Definiens Cognition Network Technology (“CNL”) is a programming environment integrated with the eCognition® OBIA software. It enables to portray the abovementioned iterative processes, making OBIA flexible enough to be applied in a wide range of image analysis fields, such as life sciences and medical image analysis (Athelogou et al., 2007; Haenschel et al., 2008). In the context of marble petrography, OBIA allows to describe and analyse mineral grain shapes in objective and comparable manner. The following sections describe the technical implementation of automated carbonate grain extraction with the eCognition® Software and aim at demonstrating the flexibility of the OBIA approach and its usability in determining marble provenance.

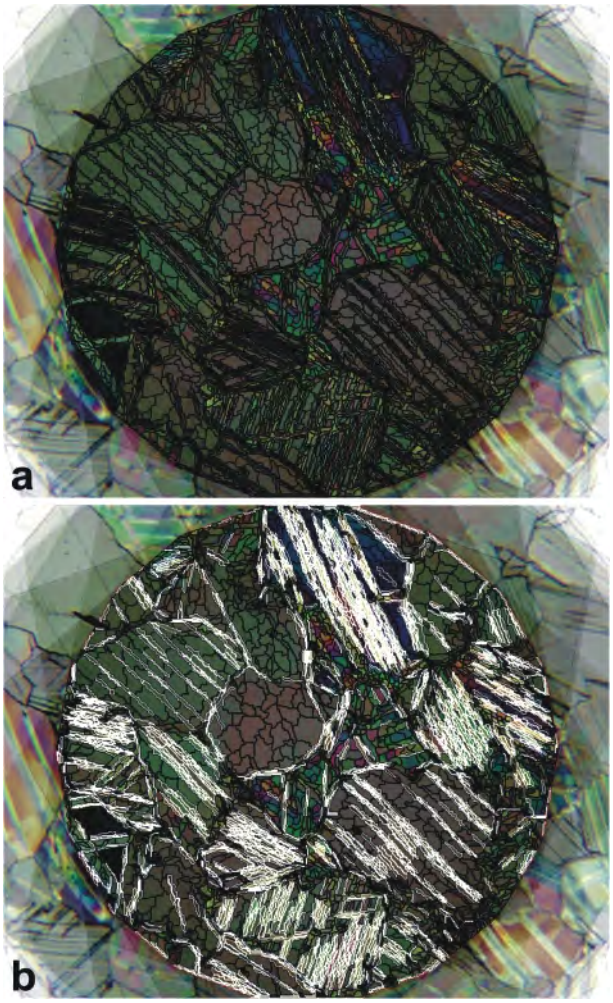

Figure 5: Re-segmentation of base level. Figure 5b: Classification of generated “internal” objects as „elongated objects“.

3.2 Strategy for analyzing the marble thin section

In the first OBIA step, which is image segmentation, we used the micrographs from all polarizations and rotation angles with equal weighting. Due to the rectangular image outline and the rotation of the specimen, peripheral areas of the image stack have incomplete image coverage. These areas were marked as background (Fig. 2a, b, c). According to the cutting angle of grain borders and thin section surface, grain borders show up differently: at some locations, grain borders are thicker than one pixel while at other locations they might be hardly visible. Consequently, treating interspaces between grains as separate objects is sensible in generating contiguous grain borders. For this purpose, a shrink-and-grow approach to generate interspace-objects was sensible, especially at locations where the grain border is hardly visible. To describe the different textures of the grains a two-level-segmentation is necessary. That means, within the boundaries of the top-level-segments sub-objects need to be created, which can then act as texture elements for their respective top-level-objects (see Fig. 3). In this particular case: delineating linear texture elements of grains as contiguous sub-objects would establish the “being-part-of” relation between grains and those lines. By characterizing the grains according to density and orientation of their linear texture elements, unwanted object borders within single grains can be dissolved.

3.3 Developing a rule set using CNL

We focused on the central circular image area where data is present in micrographs of all rotation angles. Peripheral areas were marked as background and excluded from further analysis on a quasi-pixel basis (bright translucent areas in Figs. 2, 4, 5 and 6), generated by the so-called chessboard segmentation, producing objects of one pixel size (Trimble, 2011).

The central circular area was marked as “data” area and acted as the region of interest (ROI) for any further analysis. Inside the ROI we continued our analysis by applying a two-level top down segmentation strategy.

For this purpose we were applying the multi resolution segmentation (MRS) as outlined by Baatz and Schäpe (2000): This algorithm merges neighbouring pixels or objects by maximizing within-object homogeneity and intra-object heterogeneity. The maximum allowed local heterogeneity is defined through the so-called scale parameter. The higher the scale parameter, the larger the generated objects are. The scale parameter is defined by the homogeneity of colour and shape. Both criteria can be mutually weighted (w_{shape} and w_{color}), whereas the shape criterion itself is composed by differently weighted compactness and smoothness. In this context, higher weighting com-

pactness (w_{comp}) means the object border merely follows the image contrast and thus can lead to more fringed outlines in noisy images or areas. Using the parameters as depicted in Table 1 for the MRS, initial image objects were generated as outlined in Fig. 2c.

When segmenting an image with eCognition® a hierarchical net of image objects can be generated, yielding the necessary connections for describing neighbourhood and "being-part-of" relations. In this hierarchical net of image objects, each sub-object belongs to only one super-object and the outer border of each super-object is identical to the outer borders of ist sub-objects' outer borders. (Benz et al., 2004; Fig.3). In our particular case only two initial segmentation levels were generated. The initial segmentation results are depicted in Figure 2b (top-level) and 5a (base-level).

After initial segmentation the grain borders were enhanced by growing round-shaped objects with a border index bi_v of less-equal to 1.9 by two pixels into neighbouring objects with a bi_v of more than 1.9 (Figure 4). The bi_v is defined by (Trimble, 2011):

$$bi_v = \frac{P_v}{2(w_{BB}+l_{BB})} \qquad \text{Equation (1)}$$

With: P_v the object's perimeter (border length), l_{BB} the length, w_{BB} the width of the object's smallest enclosing rectangle.

bi_v describes how jagged an object is. The higher bi_v, the more jagged an object is. In the next step, remaining elongated objects with an asymmetry *a* of more than 0.9 were deleted. The asymmetry *a* of an object is defined as the square root of the ratio between the minor and major axis of the object's minimum enclosing ellipse (Trimble, 2011):

$$a = 1 - \sqrt{\frac{\lambda_{min}}{\lambda_{max}}} \qquad \text{Equation (2)}$$

With: λ_{min}, the length of the minor axis and λ_{max} the length of the major axis of the smallest enclosing ellipse.

That means, the more elongated an object is, the closer *a* is to 1 and the less elongated an object is, the closer its value is to 0. Fig. 4a depicts the resulting segmentation. In the following step the interspace between the objects has been generated as an explicit object class. This has been done by applying the so-called pixel-based object resizing algorithm as implemented in eCognition using the shrinking mode (Trimble, 2013) for all remaining objects. The Class for new image objects then was the interspace. The Candidate Surface Tension has been set in a way, that at border positions of an object within a neighbourhood of 5x5 pixels (Box size in X and Y = 5) the relative area of the object to shrink was less-equal to 20% (Value = 0.2). The shrinking increment was limited to two pixels (Number of cycles = 2). That is, at each border position fulfilling the relative area constraint the objects of concern were shrunk by two pixels (Fig. 4b).This conditional shrinking led to more smoothed object borders than an equal shrinking. The shrunk objects were finally grown into the generated interspaces until the interspaces themselves disappeared (Fig. 4c).

So far, most of the individual carbonate grains could be delineated. Some errors in subdividing individual grains still existed, however (e.g., Fig. 4c, leftmost ellipses). In order to approximate the linear textures of the grains, the base level was

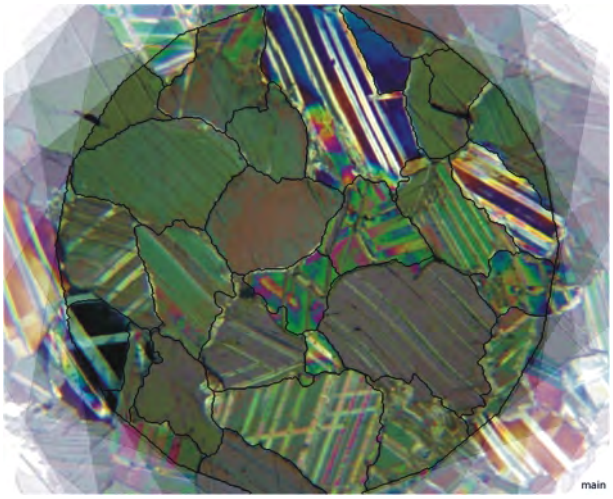

Figure 6: Delineation of grains after texture-based merging.

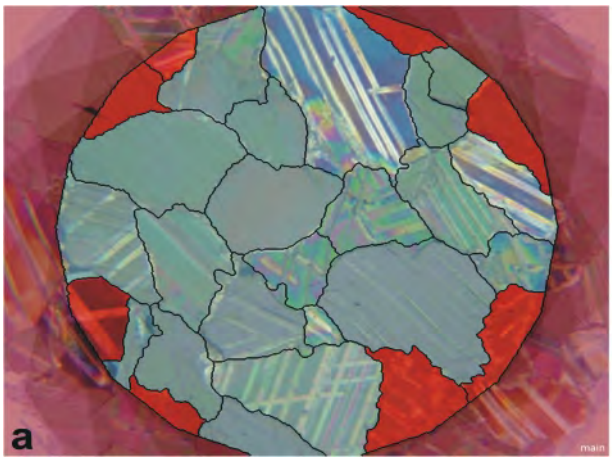

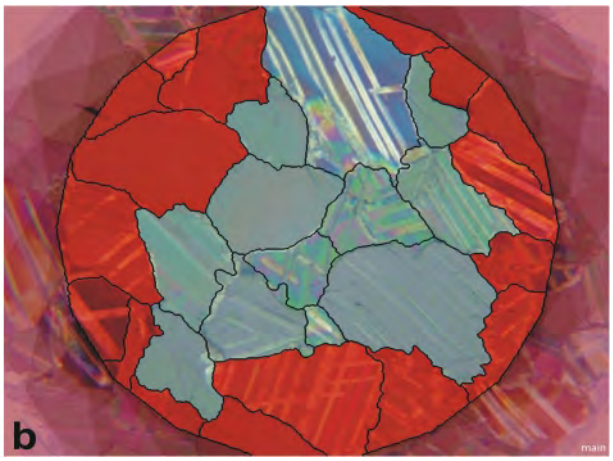

Figure 7: Enhancing grain shape statistics by step-wise exclusion of bordering grains (dark). Figure 7a (left): Grains with relative border to background of more than 30%. Figure 7b (right): bordering to background at all.

re-segmented using a MRS with the parameters as depicted in Table 2.

This way, the top-level-objects with the enhanced borders remain untouched but they contain high-resolution sub-objects (Fig. 5a). For the intended texture analysis of top-level-objects, the newly created objects at the base level were classified according to their asymmetry. That is, objects at the base level were classified as “elongated objects” (objects outlined in white, Fig. 5b) whenever their asymmetry was higher than 0.9.

Now each higher-level object refers to a number of explicitly elongated sub-objects with different main directions. That is, by referring to the density of “elongated objects” within a top-level-object these objects can be labeled as being “elongated textured”. In our case objects with more than 25% (area) of elongated sub-objects were considered “elongated textured”. Neighboring elongated textured image objects with similar orientation of their sub-objects are likely to represent one single grain with twin lamellae.

Finally, all neighboring objects on the top segmentation level with a high proportion of blue in the crosspolarized images were merged. The merging was done in order to dissolve inner grain borders produced by their lamellae structures and dis-connecting contiguous grain objects. The threshold for merging was defined by the feature “ratio blue x” (r_b^x) which has been created using the mean gray values per object. It describes the amount of the mean gray value per object in all blue channels of all crosspolarized images in relation to the mean gray values per object of all red and green channels of all cross polarized images:

$$r_b^x = \frac{\overline{b}_x}{\overline{r}_x + \overline{g}_x + \overline{b}_x} \qquad \text{Equation (3)}$$

Area([mm²])	Border length (perimeter)	Length [mm]	Length/ Width	Width [mm]	Asymmetry	Border index	Compactness	Main direction (degree)	Shape Index
0.75	4.95	1.19	1.25	0.96	0.48	1.42	1.53	151.97	1.43
0.16	2.39	0.78	2.31	0.34	0.69	1.39	1.69	108.87	1.51
0.25	3.18	0.71	1.12	0.63	0.19	1.57	1.75	15.89	1.58
0.07	1.82	0.56	3.00	0.19	0.84	1.52	1.57	124.72	1.77
0.50	3.95	1.03	1.35	0.76	0.41	1.38	1.56	105.20	1.39
0.08	2.06	0.59	2.00	0.29	0.81	1.69	2.12	17.27	1.80
0.22	2.91	0.84	1.73	0.49	0.48	1.50	1.89	154.25	1.56
0.16	2.91	0.85	2.77	0.31	0.79	1.59	1.61	23.59	1.81
0.29	3.41	0.72	1.02	0.70	0.11	1.56	1.71	140.31	1.57
0.05	1.20	0.28	1.00	0.28	0.37	1.37	1.65	147.29	1.38
0.30	3.32	0.87	1.67	0.52	0.44	1.47	1.52	166.49	1.52
0.15	2.00	0.56	1.44	0.38	0.50	1.28	1.46	161.38	1.31
0.68	4.76	1.15	1.37	0.84	0.31	1.42	1.43	115.45	1.45
0.16	2.38	0.58	1.14	0.51	0.12	1.48	1.88	87.11	1.50
0.14	2.08	0.51	1.25	0.41	0.20	1.37	1.46	91.16	1.38
0.34	3.50	0.96	1.50	0.64	0.49	1.47	1.83	151.66	1.51
0.36	3.12	0.83	1.26	0.66	0.29	1.28	1.52	74.53	1.29
0.24	2.78	0.71	1.18	0.60	0.14	1.41	1.78	104.54	1.42
0.23	2.87	0.92	2.56	0.36	0.78	1.34	1.44	136.72	1.50
0.28	3.42	0.87	1.89	0.46	0.61	1.53	1.42	139.26	1.61
0.49	3.82	1.07	1.52	0.71	0.41	1.33	1.56	86.42	1.37
0.18	2.38	0.61	1.34	0.46	0.21	1.37	1.51	152.39	1.39
0.12	2.14	0.63	1.86	0.34	0.68	1.44	1.71	155.38	1.52
0.31	3.19	0.78	1.14	0.68	0.41	1.43	1.72	36.30	1.44
0.15	2.65	0.86	2.64	0.33	0.78	1.50	1.81	145.12	1.69
0.11	2.26	0.62	1.69	0.37	0.64	1.61	2.03	46.11	1.68
0.10	1.76	0.42	1.05	0.40	0.24	1.37	1.69	154.67	1.39
0.08	1.99	0.69	3.31	0.21	0.85	1.51	1.88	115.97	1.80
0.06	1.38	0.40	1.94	0.21	0.58	1.37	1.46	43.01	1.46

Table 3: Shape describing parameters of top-level objects (carbonate grains).

With: $\overline{r}_x$ the mean gray value within an object of the red channels of all cross polarized images; $\overline{g}_x$ the mean gray value within an object of the green channels of all cross polarized images; $\overline{b}_x$ the mean gray value within an object of the blue channels of all cross polarized images;

That means, the higher the amount of the blue channels in relation to the red and green channels of the cross polarized images, the higher r_b^x is. For the color mixing as displayed in Figure 2, bluish objects have a relatively high value of $r_b^x \geq 0.3$, since the sum of all color proportions must be at 1.0. Respectively, the threshold for merging neighboring objects has been set to $r_b^x \geq 0.32$. The result of texture-based merging is shown in Fig. 6.

3.4 Analysis of detected grains

For an elaborated analysis of thin sections a statistical evaluation of shape describing parameters of the delineated grains is essential. In our case, the basis for statistical analysis of marble sample LAS3 was the segmentation result displayed in Figure 6. For a statistical characterization of the sample by grain shapes we used the following object features: area [mm²], border length [mm], length [mm], width [mm], ratio of length to width, main direction [degree], border index (equation (1)) and asymmetry (equation (2)). In eCognition, all of them are generated automatically per object. That is, for each grain respective values are generated. Additionally, we included shape describing parameters in the statistical analysis: shape index si_v and compactness c_v. Both are already implemented in eCognition: (Trimble, 2011):

$$si_v = \frac{P_v}{4\sqrt{A_v}} \qquad \text{Equation (4)}$$

With: P_v the object perimeter, A_v the object area. si_v describes the smoothness of an object's shape. The smoother an object shape is, the lower si_v is. The compactness is similar to the border index, but its calculation is based upon the object area. The higher c_v is, the less compact an object is.

$$c_v = \frac{l_v \cdot w_v}{A_v} \qquad \text{Equation (5)}$$

With: A_v the object area, l_v the length, w_v the width of the object.

Some of the segmented grains cross the border between ROI and background. In consequence, including their shape parameters would distort overall sample statistics. Defining objects as "cut" whose shared border to background is longer than 30% of their overall border while objects below this threshold are not significantly cut (Fig. 7a), reduced the sample size from 29 to 21 grain objects. Excluding all objects bordering to background would reduce the number of samples to 12 grain objects (Fig. 7b, Table 4).

4. Results

Table 3 gives the shape parameters as mentioned above for all segmented grains. Comparing the results on grain length with that of 100 manual measurements of the same sample shows only little deviation: the mean grain length from manual measurement is at 0.7 mm (section 2.3) while the mean grain length derived from OBIA is at 0.74 mm for all objects and those being uncut by the border. For all grains including those with a common border to background of < 30% of the whole grain border, the mean length is at 0.78 mm (Table 4). The maximum grain length determined by manual analysis is given with 1.3 mm while in Table 3 the maximum grain length determined with OBIA is at 1.19 mm.

5. Conclusions

While our approach is certainly just one among the numerous recently available and promising methods, the results of this OBIA feasibility study indicate clear advantages over the manual approach and over conventional methods of petrographic image analysis. For an experienced expert the manual determination of size for 100 grains can be estimated about 1 h. Image acquisition time for 36 images per sample can be estimated as approx. five minutes on a standard petrographic microscope. The results on maximum and average grain lengths achieved with OBIA are consistent with the results of manual measurements (section 2.3, Tables 3 and 4). Assuming the developed OBIA rule set needs no manual adaptations, producing respective results for further similar specimen is a matter of a few seconds per thin section on a standard PC. The segmentation is transparent and easily adaptable to varying imaging conditions (Hofmann, 2008). With OBIA, carbonate mineral grains can be reliably represented as a hierarchy of grain objects and sub-objects like inclusions, twin-lamellae etc. Once grain objects have been extracted, characteristic grain shape parameters can be automatically gauged. Further potentials for OBIA in the field of thin section analysis are given by the extended shape-relevant measures like grain area, asymmetry or border index of the grains as well as fabric-relevant parameters like the main anisotropy. Different types of minerals

	n	Area [mm²]	Border length (perimeter) [mm]	Length [mm]	Length/ Width	Width [mm]	Asymmetry	Border index	Compactness	Main direction (degree)	Shape Index
all	29	0.24	2.78	0.74	1.70	0.48	0.48	1.45	1.66	108.73	1.52
no border	12	0.26	2.89	0.74	1.41	0.53	0.34	1.44	1.64	130.64	1.47
Border < 30%	21	0.28	2.97	0.78	1.50	0.54	0.41	1.43	1.65	117.96	1.47

Table 4: Mean values of shape describing features for objects with different shared border length to "background".

can be distinguished, enabling stratified statistical analysis (Marschallinger and Hofmann, 2010). Summing up, OBIA is a state-of-the-art method to deliver objective and traceable mineral shape parameters from petrographic micrographs in a highly automated manner. It is considered a powerful component not only in the multidisciplinary toolbox for designating marble provenance, but for automated petrographic (i.e. micro texture) analysis from thin sections in general. Since the rule set developed here can be reused, OBIA has the potential to drastically accelerate thin section analysis.

References

Athelogou, M., Baatz, M., Binnig, G., Schäpe, A., Schmidt, G., 2007. Definiens Cognition Network Technology – A Novel Multimodal Image Analysis Technique for Automatic Identification and Quantification of Biological Image Contents. In: Frischknecht, F., Shorte, S.L., (Eds.): Imaging Cellular and Molecular Biological Functions, Springer. Berlin, Heidelberg. pp. 407-421.

Attanasio, D., 2003. Ancient white marbles: analysis and identification by paramagnetic resonance spectroscopy. L'Erma di Bretschneider, Roma, pp. 1-283.

Baatz, M., Hoffmann, C. Willhauck, G., 2008. Progressing from object-based to object-oriented image analysis. In: Blaschke, Th., Lang, S., Hay, G.J. (Eds.): Object-Based Image Analysis. Spatial Concepts for Knowledge-Driven Remote Sensing Applications. Springer. Berlin, Heidelberg, pp. 29–42.

Baatz, M., Schäpe, A., 2000. Multiresolution segmentation: An optimization approach for high quality multi-scale image segmentation. In: Strobl, J., Blaschke, T., Griesebner, G. (Eds.): Angewandte Geographische Informations –Verarbeitung, Wichmann: Karlsruhe; Volume XII,12–23.

Benz, U., Heynen, M., Hofmann, P., Lingenfelder, I., Willhauck, G., 2004. Multi-resolution, object-oriented fuzzy analysis of remote sensing data for GIS-ready information. In: ISPRS Journal of Photogrammetry & Remote Sensing, 239-258.

Blaschke, T., 2010. Object based image analysis for remote sensing. In: ISPRS International Journal of Photogrammetry & Remote Sensing 65 (1), 2-16.

Blaschke, T., Strobl, J., 2001. What's wrong with pixels? Some recent developments interfacing remote sensing and GIS. GIS-Zeitschrift für Geoinformationssysteme 6, 12–17.

Bons, P., Jessell, M.W., 1996. Image Analysis of Microstructures in Natural and Experimental Samples. In: De Paor, D. G. (Ed.): Structural Geology and Personal Computers. Pergamon, pp. 135-166.

Craig, H. and Craig, V., 1972. Greek Marbles: Determination of Provenance by Isotopic Analysis, Science, 176, 401-403.

Cramer, T., 2004. Multivariate Herkunftsanalyse von Marmor auf petrographischer und geochemischer Basis. http://opus.kobv.de/tuberlin/volltexte/2004/742/pdf/cramer_thomas.pdf. (last access: 05 May 2013).

Erdas, 2011. Imagine AutoSync, http://www.erdas.com (last access: 05 May 2013).

Fueten, F., 1997. A computer-controlled rotating polarizer stage for the petrographic microscope. Computers & Geosciences, 23/2, 203-208.

Gorgoni, C., Lazzarini, L., Pallante, P., 2002. New archaeometric data on «Rosso Antico» and other red marbles used in antiquity. In L. Lazzarini (ed.), «ASMOSIA VI, Interdisciplinary Studies in Ancient Stone», Padova, pp. 199-206.

Haenschel, C., Linden, D., Oertela, V., Rotarska-Jagiela, A., Schönmeyer, R., Vogeley, K. 2008. The corpus callosum in schizophrenia - volume and connectivity changes affect specific regions. NeuroImage, 39/4, 1522-1532.

Herz, N., 1988. The oxygen and carbon isotopic data base for classical marble; in: Herz, N. and Waelkens, P., Classical Marble: Geochemistry, Technology, Trade, Kluwer Academic Publishers, pp. 305-314.

Higgins, D.D., 2006. Quantitative Textural Measurements in Igneous and Metamorphic Petrology. Cambridge University Press, 265p.

Hofmann, P., Strobl, J., Blaschke, T., 2008. A Method for adapting global image segmentation methods to images of different resolutions. In: Hay, G.J., Blaschke T. and Marceau D. (Eds). GEOBIA 2008 – Pixels, Objects, Intelligence. GEOgraphic Object Based Image Analysis for the 21st Century. University of Calgary, Calgary Alberta, Canada, August 05-08. (International Archives of the Photogrammetry, Remote Sensing and Spatial Inf. Sciences Vol. XXXVIII-4/C1).

Lang, S., 2008. Object-based image analysis for remote sensing applications: modeling reality – dealing with complexity. In: Blaschke, T., Lang, S., Hay, G.J. (Eds.): Object-Based Image Analysis. Spatial Concepts for Knowledge-Driven Remote Sensing Applications. Springer, pp. 3-27.

Lazzarini, L., 2004. Archaeometric aspects of white and coloured marbles used in antiquity: the state of the art. Periodico di Mineralogia (2004), 73, 113-125.

Lepsius, R.,1891. Griechische Marmorstudien, Abhandlungen Königl. Akademie der Wissenschaften, Phil.-Hist. Klasse 1890, Berlin, 1-135.

Marschallinger, R. and Hofmann, P., 2010. The application of Object Based Image Analysis to Petrographic Micrographs. In: Mendez-Vilas, A. and Diaz, J. (Eds.): Microscopy: Science, Technology, Applications and Education, Vol. 4, pp. 1526-1532. Formatex Research Center.

Obara, B., Kozusnikova, A., 2007. Utilisation of the image analysis method for the detection of the morphological anisotropy of cacite grains in marble. Computational Geosciences 11, 275-281.

Trimble, 2011. eCognition® Developer 8.64.1 Reference Book. Trimble Germany.

Tröger, W., Bambauer, H-U., Taborszky, F., Trochin, H., 1982. Optische Bestimmung der Gesteinsbildenden Minerale, Teil 1 Bestimmungstabellen. Schweizerbart, Stuttgart, 188 p.

Unterwurzacher, M. & Obojes, U., 2012. White marble from Laas (Lasa), South Tyrol – its occurrence, use and petrographic-isotopical characterization. Austrian Journal of Earth Sciences, 105/3, 26-37.

Unterwurzacher, M., Pollerers, J., Mirwald, P.W., 2005. Provenance study of marble artefacts from the Roman burial area of Faschendorf (Carinthia, Austria). Archaeometry 47, 265-273.

Received: 9 May 2013
Accepted: 10 October 2013

Peter HOFMANN[1)*], Robert MARSCHALLINGER[1)], Michael UNTERWURZACHER[2)3)] & Fritz ZOBL[1)]

[1)] Interfaculty Department of Geoinformatics, University of Salzburg, Schillerstr. 30, 5020 Salzburg, Austria;

[2)] Department of Geography and Geology, University of Salzburg, Hellbrunnerstr. 34, 5020 Salzburg, Austria;

[3)] Institute of Archaeology, University of Innsbruck, Langer Weg 11, 6020 Innsbruck, Austria;

[*)] Corresponding author, peter.hofmann@sbg.ac.at